FINITE DIFFERENCE ANALYSIS OF GREY CAST-IRON SOLIDIFICATION PROCESS

V.S.R. Murthi
Additional Controller
JNTU College of Engineering
Kukatpally; Hyderabad- 500 072

A. CHENNAKESAVA REDDY
Associate professor
Department of Mechanical Engineering
JNTU College of Engineering
Kukatpally; Hyderabad – 500 072

Abstract: *This article describes the solidification process of grey cast iron using finite difference method. Two models are formulated for the solidification process. The computed results are compared with the experimental results. The important conclusions are: (i) During the solidification process, the cooling rate and undercooling are two important factors influencing the formation of the microstructure and heat transfer and (ii) A higher cooling rate yields a higher level of undercooling, which results in greater grain density and a smaller grain radius.*

1. INTRODUCTION

For binary alloys, macro-models based on phase diagrams are generally used to solve solidification problems [1]. These models can give only rough predictions of the solidification time, isotherms etc., which do not have any direct relation with the microstructures and physical properties of solidified alloys. Recently, the micro-viewpoint has gradually been incorporated into the solidification models. In these models, the microstructure evolution during the solidification process is considered. The whole process includes three different steps: nucleation (an increase in the number of nuclei), growth (an increase in the volume of the grain) and impingement [2].

In the solidification process, as the temperature of the liquid metal falls below the melting point, nucleation begins, and then crystal clusters are formed. These clusters may melt or grow. When the clusters are big enough, they will not melt any more. At this time, they are called nuclei. At the beginning of nucleation, the number of nuclei increases very slowly. After a critical undercooling value is reached (ΔT_n), the number increases rapidly. Nucleation proceeds until the decreasing temperature starts to increase. At this point, the number of nuclei reaches its maximum value [3,4]. After nucleation, there is a long period of growth. In this step, the grain radii increase continuously until the grains come into contact with one another, and this is followed by the third step: impingement. In the final step, though the grain radii cannot increase any more, there is still some liquid metal among or inside the grains, which will solidify in this step.

This paper focuses on equiaxed eutectic solidification, and the testing alloy is grey cast iron. A solidification problem of a cylindrical casting is solved by using the following two models:

- Nucleation is assumed to occur instantaneously.
- The Gaussian distribution is used in the nucleation step, and the Close-Pack model is applied to the final step.

2. MATHEMATICAL MODELS AND FINITE DIFFERENT METHOD

Two macro-micro models are built to simulate the equiaxed solidification of gray cast iron. A cylindrical casting as shown in Fig.1 is used. The following assumptions are made to build the models:

- There is no melt flow during the solidification process.
- The grain shape during nucleation and growth is spherical.
- The testing cylinder is axi-symmetric.

The energy equation is

$$\rho c_p \frac{\partial T}{\partial t} = k\left[\frac{\partial^2 T}{\partial r^2} + \frac{1}{r}\frac{\partial T}{\partial r} + \frac{\partial^2 T}{\partial z^2}\right] + \rho L \frac{\partial f_s}{\partial t} \qquad \ldots(1)$$

where c_p is the specific heat, ρ is the density, k is the thermal conductivity, L is the latent heat and f_s is the local volume fraction of the solid.

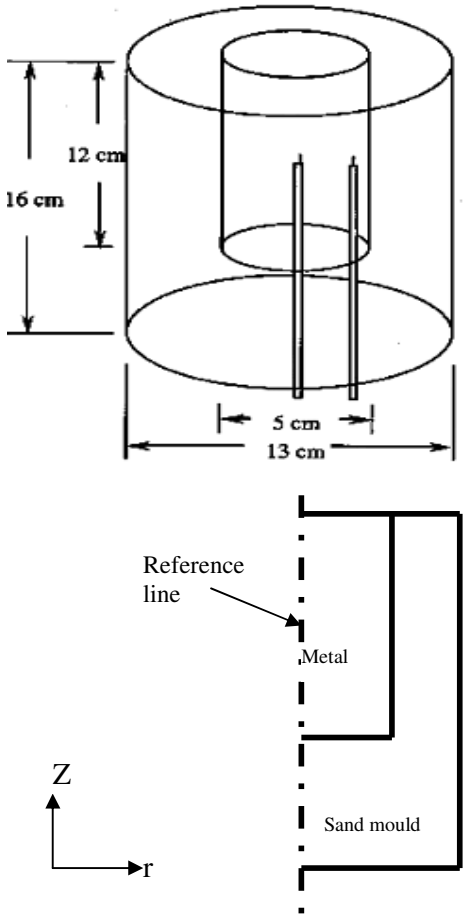

Fig.1 A schematic figure of cylindrical test casting

The initial condition is:

$T(r, z, t=0) = T_o$ …(2)

Where T_0 is the pouring temperature of the liquid metal

The boundary conditions are:

- At the center (reference) line ($r = 0$)

$$\left.\frac{\partial T}{\partial r}\right|_{r=0} = 0 \qquad ...(3)$$

- At the air/metal interface (z = 16 cm)

$$q'' = h(T - T_\infty) \qquad ...(4)$$

where q'' is the heat flux, h is the convective heat transfer coefficient of air, T_∞ is the atmospheric temperature.

- At the metal/mould interface

$$q'' = h_{equi}(T - T_\infty) \qquad ...(5)$$

where h_{equi} is the equivalent heat transfer coefficient of the sand mould.

Local volume fraction of solid, $f_x(t) = \frac{4}{3}\pi R^3(t)N(t)$ ...(6)

Where N(t) is grain number per unit volume and R(t) is the grain radius.

The derivative of f_s is written as

$$\frac{df_s}{dt} = 4\pi R^2(t)N(t)\frac{dR}{dt} + \frac{4}{3}\pi R^3(t)\frac{dN}{dt} \qquad ...(7)$$

Because the radius is very small in the nucleation, the second term on the right hand side of equation (7) can be ignored, and the equation is written as

$$\frac{df_s}{dt} = 4\pi R^2(t)N(t)\frac{dR}{dt} \qquad ...(8)$$

Equations are the basic equations of the micro-macro models.

2.1 *Model – 1*

In this model, the nucleation is assumed to occur instantaeously. This means that the nucleation step does not need to be considered, and that N(t) is a constant. Accordingly, equations (6) and (8) are rewritten as

$$f_x(t) = \frac{4}{3}\pi R^3(t)N \qquad ...(9)$$

$$\frac{df_s}{dt} = 4\pi R^2(t)N\frac{dR}{dt} \qquad ...(10)$$

in the growth step, the growth rate V can be given by

$$V = \mu (\Delta T)^2 \qquad ...(11)$$

The μ is a growth constant and ΔT is the undercooling.

$$\Delta T = T_e - T \qquad ...(12)$$

where T_e is the eutectic temperature.

The radius of the nucleus is obtained by integrating equation (11)

$$R = r_0 + \int_0^t \mu[(T_e - T(t))]dt \qquad \ldots(13)$$

Where r_0 is the critical radius.

For the impingement step, the equation (10) is modified as

$$\frac{df_s}{dt} = 4\pi R^2(t) N \frac{dR}{dt} f_s \qquad \ldots(14)$$

by integrating equation (14),

$$f_s(t) = 1 - \exp\left[- N \frac{4}{3} \pi R^3(t) \right] \qquad \ldots(15)$$

2.2 *Model – 2*

In this model, the Gaussian distribution is used to capture the variation in the trend of the nucleation rate. The equation for dN/dt can be written as

$$\frac{dN}{dt} = \frac{N_{\max}}{\sqrt{2}\Delta T_\sigma} \exp\left[\frac{-(\Delta T - \Delta T_\sigma)^2}{2\Delta T_\sigma} \right] \frac{dT}{dt} \qquad \ldots(16)$$

where ΔT_0 is the undercooling at the tip point of the Gaussian distribution, ΔT_σ is the standard deviation of the distribution, and N_{max} is the total grain density of the whole distribution (integrating Eq. (16) from zero undercooling to infinity). When $\partial T/\partial t > 0$ (i.e., the recalescence occurs), $dN = 0$. This is the end point of the nucleation step. In the growth step, equation (11) is also used to calculate the grain radius. The two-step Close-Pack model is applied in the impingement step, and the f_s is given by

$$\frac{df_s}{dt} = \phi 4\pi R^2(t) N(t) \frac{dR}{dt} \qquad \ldots(17)$$

$$\phi = \begin{cases} -10.32 \log_{10}(f_s) & 1 \geq f_s \geq 0.8 \\ 1 & f_s \leq 0.8 \end{cases} \qquad \ldots(18)$$

The finite difference method is used to compute the temperature distribution. While formulating the finite difference equations, the central difference is used for the space derivative, and the backward difference is used fir the time derivative. The algebraic equations are solved using **MATLAB** software package.

3. RESULTS AND DISCUSSION

The testing material is gray cast iron, whose microstructure is equiaxed eutectic. The node number of the uniform grid used in the computation is 61 X 26. In Model – 1 the time step was 1.0 second and in Model - 2 the step was 0.1 second. For convenience, the center point of the casting is used as a reference point.

Fig.2 shows the computational and experimental cooling curves of the reference point. From this, it can be found that the computational data of the cooling curve and undercooling are quite close to the experimental data. Fig.3 illustrates the cooling curves of Model - 1and Model - 2. Though these two models are quite different from each other, the computational results are very similar. In case of Model – 2, there is a small degree of recalescence (or the maximum undercooling), which is closer to the experimental result.

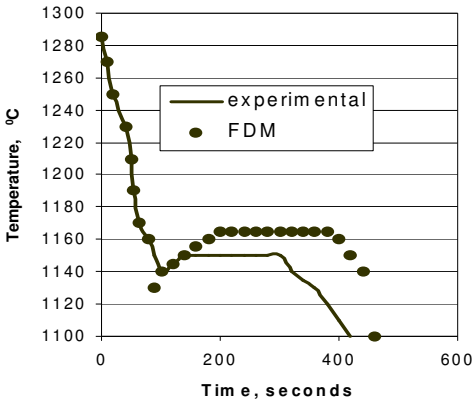

Fig.2 The cooling curves from the experiment and finite difference model

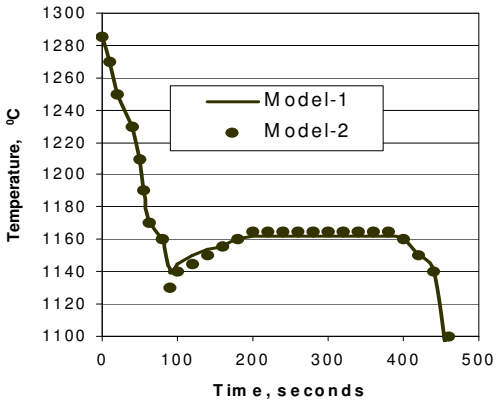

Fig.3 The cooling curves obtained by the Finite difference models

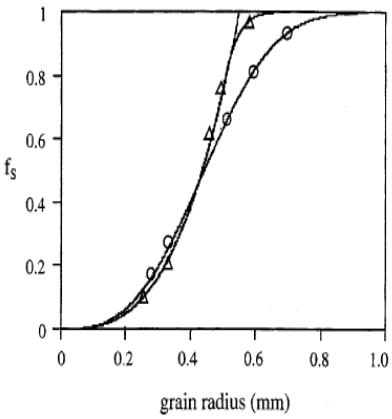

Fig.4 f_s v/s the grain for different models

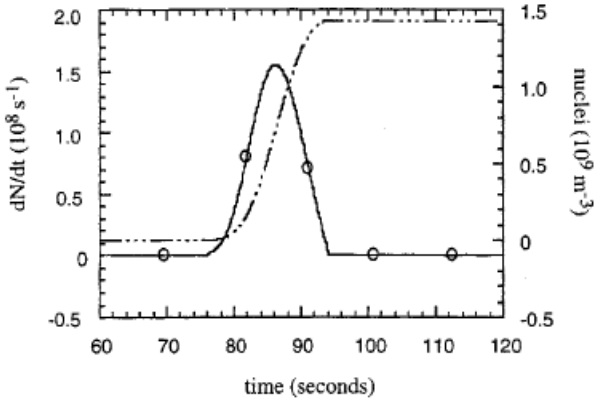

Fig.5 The nucleation rate and gain density distribution

Fig.4 shows f_s v/s the grain radius at the centerline for Model –1 and Model –2. In Model –1, since f_s increases slowly and smoothly with the grain radius, the larger time step can be used, and the convergence rate is faster than that in Model -2. However, in Model –1, f_s will not be one until the radius reaches infinity. This is not reasonable. Accordingly, the end point of solidification is set at the radius when $f_s = 0.999$. At the reference point, the relationship between the nucleation rate (or grain density) and time is that shown in Fig.5. In the figure, it is shown that the Gaussian distribution can successfully simulate the big change of the nucleation rate in a short time. After the nucleation step, the grain density reaches a constant value, i.e., the final grain density. It can also be found that the nucleation time (about 18 seconds) is very short compared to the local solidification time (about 300 seconds). This proves that the assumption of instantaneous nucleation is reasonable.

In general, it is thought that a higher cooling rate (dT/dt) yields a higher grain density since the higher cooling rate leads to greater undercooling, which results in a larger number of nuclei. This is consistent with the computed results. In Fig 6-7, the distributions of the maximum undercooling, grain density and radius of Model -2 are shown. From these figures, it can be found the grain radius is strongly related to the undercooling. Closer to the center point (where the cooling rate is lower), the maximum level of undercooling is lower, the grain radius is larger.

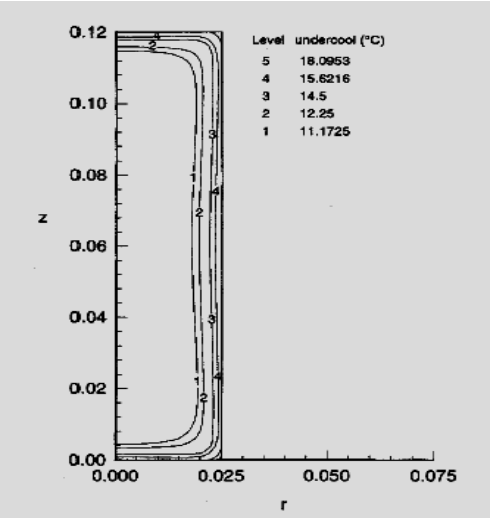

Fig.6 The temperature distribution during undercooling

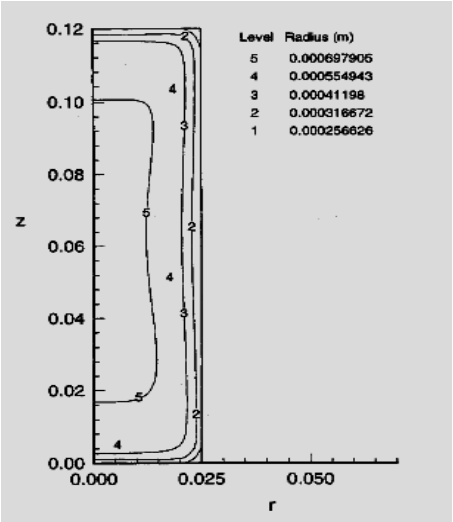

Fig.7 The grain size distribution after solidification

From this study, it can also be seen that the advantages of Model –1 are that the formulation is simple, and that the undercooling prediction is not bad. However, Model -1 cannot obtain the nucleation rate or the grain density, which varies with time, and the grain radius should be infinite, which would make f_s equal to one, which is not reasonable. Therefore, Model -1 is only suitable for rough evaluation of the solidification process. On the other hand, Model -2 can obtain more information about solidification and a better undercooling prediction than can Model -1. However, the computation for Model -2 is not very stable, so a small time step is needed. The convergence rate of each time step is also low. Consequently, Model -2 uses much more computation time than does Model -1.

4. CONCLUSIONS

The important conclusions are:

- During the solidification process, the cooling rate and undercooling are two important factors influencing the formation of the microstructure and heat transfer.
- A higher cooling rate yields a higher level of undercooling, which results in greater grain density and a smaller grain radius.
- By using model –1 or –2, the cooling curves and undercooling can be predicted.
- The formulation of the model –1 is simple and the convergence rate is fast.
- The nucleation rate, grain density and radius, which vary with time, can be obtained using Model –2. These cannot be obtained using Model –1.

5. REFERENCES

1. M. Rappaz, Modeling of microsturcture formation in solidification processes, International Materials Reviews, 34 (1989), p93
2. T.C. Tszeng, Y.T. Im, and S.Kobayashi, Thermal analysis of solidification by the temperature recovery method, International Journal of Machine Tools and Manufacturing, 29 (1989), p107
3. J.S. Hsiao, An efficient algorithm for finite difference analysis of heat transfer with melting and solidification, International Journal of Numerical Heat Transfer, 8(1985), p653
4. V.R. Voller and R. Swa, General source based method for solidification phase change, International Numerical Heat Transfer, Part B, 19(1991), p175